LM-06K007
February 14, 2006

A General Method for Calculating the External Magnetic Field from a Cylindrical Magnetic Source using Toroidal Functions

J Selvaggi, S Salon, O Kwon and CVK Chari

A General Method for Calculating the External Magnetic Field from a Cylindrical Magnetic Source using Toroidal Functions

J. Selvaggi, Dr. S. Salon, Dr. O. Kwon, and Dr. M.V.K. Chari
Electrical, Computer, and Systems Engineering Department Rensselaer Polytechnic Institute
Troy, NY 12180-3590

ABSTRACT

An alternative method is developed to compute the magnetic field from a circular cylindrical magnetic source. Specifically, a Fourier series expansion whose coefficients are toroidal functions is introduced which yields an alternative to the more familiar spherical harmonic solution or the Elliptic integral solution.

This alternate formulation coupled with a method called charge simulation allows one to compute the external magnetic field from an arbitrary magnetic source in terms of a toroidal expansion. This expansion is valid on any finite hypothetical external observation cylinder. In other words, the magnetic scalar potential or the magnetic field intensity is computed on a exterior cylinder which encloses the magnetic source. This method can be used to accurately compute the far field where a finite element formulation is known to be inaccurate.

INTRODUCTION

A method using a Fourier series expansion, derived from the free-space Green's function in cylindrical coordinates, will be used to characterize the external magnetic field from a circular cylindrical magnetic source. This method can be employed for computing the near-field or the far-field solution from any source which exhibits circular cylindrical symmetry. It is quite useful for computing the far-field solution when other methods, such as finite element analysis, are not very accurate.

If the geometry of the source is not cylindrical, then a particular technique called *charge simulation* illustrated in Kwon *et al.* (2004) and Schwab (1988) is used to replace the arbitrary magnetic source with fictitious magnetic point charges on a finite circular cylinder. Charge simulation is a method by which a configuration of simulation charges is determined, and whose potential function or field function approximates the true potential or field of the actual electric or magnetic source. The first type of charge simulation is that derived from a known electric or magnetic scalar potential function, and the second type of charge simulation is that derived from experimental data such as the normal component of the magnetic flux density measured on a closed hypothetical cylinder surrounding a real magnetic source. This paper will consider the former.

FORMULATION

Assume that a magnetic scalar potential can be computed close to the magnetic source. For example, a finite element analysis is most useful for computing the magnetic scalar potential on a hypothetical boundary enclosing an arbitrary source. This has been done by Kwon (2004). Consider the simplified model shown in Figure 1.

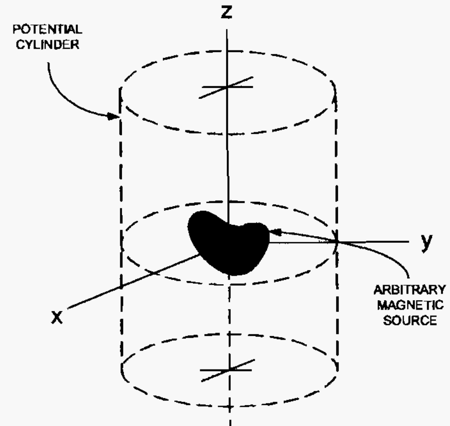

FIGURE 1 Potential cylinder

Compute the magnetic scalar potential on a chosen grid of points lying on the hypothetical cylinder. The hypothetical cylinder will be called the *potential cylinder*. The basic idea of charge simulation for a magnetic system is to replace the actual magnetic source with a new source made up entirely of fictitious magnetic point charges which yields the same computed potentials on the potential cylinder as the original source did. This is shown in Figure 2.

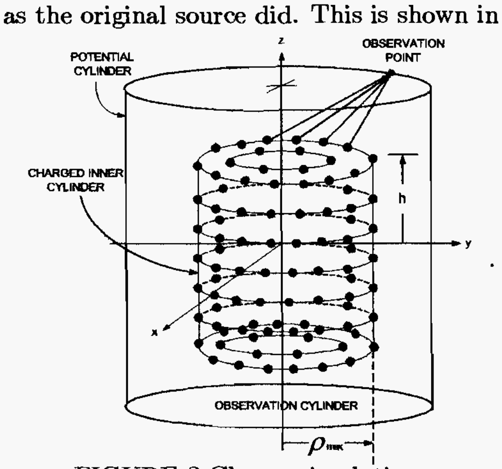

FIGURE 2 Charge simulation

The *charge cylinder* completely encloses the actual source, but lies inside the potential cylinder. Once the charge cylinder is found which reproduces the correct potentials on the potential cylinder, then one can use the charge cylinder and the magnetic form of Coulomb's law given in Stratton (1941) to compute the magnetic scalar potential external to this new source. In contrast to finite-difference and finite-element methods, the charge simulation method is well suited for unbounded electromagnetic problems, but can be modified to handle bounded problems. The hypothetical surface used in charge simulation could be any closed surface surrounding the real source. However, choosing the appropriate geometry that fits the particular problem may simplify the analysis.

In order to perform the charge simulation method, one must formulate the correct mathematical steps. One can write the magnetic form of Coulomb's law in matrix form as

$$\begin{bmatrix}\Phi_1\\ \Phi_2\\ \vdots\\ \Phi_n\end{bmatrix} = \frac{1}{4\pi}\begin{bmatrix}\frac{1}{r_{11}} & \frac{1}{r_{12}} & \cdots & \frac{1}{r_{1n}}\\ \frac{1}{r_{21}} & \frac{1}{r_{22}} & \cdots & \frac{1}{r_{2n}}\\ \vdots & \vdots & \ddots & \vdots\\ \frac{1}{r_{n1}} & \frac{1}{r_{n2}} & \cdots & \frac{1}{r_{nn}}\end{bmatrix}\begin{bmatrix}\Omega_1\\ \Omega_2\\ \vdots\\ \Omega_n\end{bmatrix} \tag{1}$$

where Φ is the magnetic scalar potential, r is the distance between the source point and the field point, and Ω is the fictitious charge. It is necessary to choose a grid with enough points so that an accurate reproduction of the original computed potentials can be established. This involves a bit of trial-and-error. There appears to be no easy way to predict how many charges would be necessary to produce an accurate potential function a' priori. This is not based on any known mathematical law, but on the authors research and is subject to change. In order to compute the charges, one needs to compute the inverse of the $\frac{1}{r_{ij}}$ matrix as shown in (1). The inversion process could take some time because the number of potential points could be large in number.

$$\begin{bmatrix}\Omega_1\\ \Omega_2\\ \vdots\\ \Omega_n\end{bmatrix} = 4\pi\begin{bmatrix}\frac{1}{r_{11}} & \frac{1}{r_{12}} & \cdots & \frac{1}{r_{1n}}\\ \frac{1}{r_{21}} & \frac{1}{r_{22}} & \cdots & \frac{1}{r_{2n}}\\ \vdots & \vdots & \ddots & \vdots\\ \frac{1}{r_{n1}} & \frac{1}{r_{n2}} & \cdots & \frac{1}{r_{nn}}\end{bmatrix}^{-1}\begin{bmatrix}\Phi_1\\ \Phi_2\\ \vdots\\ \Phi_n\end{bmatrix} \tag{2}$$

One can now expand the potential of a unit point charge in terms of the free-space Green's function expansion given by Jackson (1999), Smythe (1968), and Bouwkamp and Bruijn (1947). In cylindrical coordinates, the free-space Green's function leads to an expression for the inverse distance between the source point and the field point as shown in Figure 3.

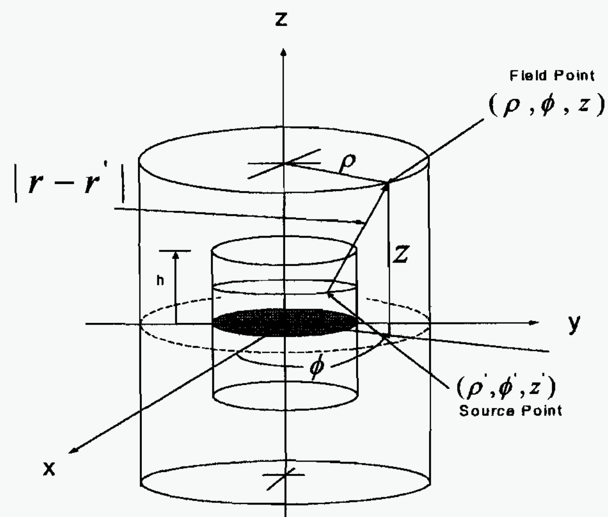

FIGURE 3 The circular cylindrical model

The inverse distance is given by

$$\frac{1}{|\mathbf{r}-\mathbf{r}'|} = \frac{1}{\sqrt{\rho^2 + a^2 + z^2 - 2a\rho\cos(\phi - \phi')}}. \tag{3}$$

This relation for the inverse distance can be written in terms of a Fourier series expansion whose weighting coefficients are the Legendre functions of the second kind and of half-integral degree. These are also called toroidal functions of zeroth order found in Lebedev (1965) or Q-functions found in Snow (1952), Snow (1949) and in Hobson (1900). The expansion is given by

$$\begin{aligned}\frac{1}{|\mathbf{r}-\mathbf{r}'|} &= \frac{1}{\pi\sqrt{\rho\rho'}}\sum_{m=0}^{\infty}\epsilon_m Q_{m-\frac{1}{2}}(\xi)\bullet\\ &\quad \cos\left[m\left(\phi - \phi'\right)\right],\end{aligned} \tag{4}$$

Equation (4) is the essential ingredient for calculating the magnetic scalar potential external to a circular cylindrical magnetic source where $\xi = \frac{\rho^2+\rho'^2+(z-z')^2}{2\rho\rho'} > 1$, ϵ_m is 1 for $m = 0$, and $\epsilon_m = 2\ \forall\ m \geq 1$. It was shown by Selvaggi *et al.* (2004) that

$$\begin{aligned}Q_{m-\frac{1}{2}}(\xi) &= \frac{\pi}{(2\beta_k)^{m+\frac{1}{2}}\,2^m}\sum_{n=0}^{\infty}\frac{(4n+2m-1)!!}{2^{2n}(n+m)!n!}\bullet\\ &\quad \frac{1}{(2\xi)^{2n}}.\end{aligned} \tag{5}$$

When a magnetic field is produced from an arbitrary source, the application of charge simulation along with the magnetic form of Coulomb's law will allow one to compute the magnetic field external to an equivalent cylindrical source. Coulomb's law for hypothetical magnetic charges is shown by Stratton (1941) to be

$$\Phi_P(\rho, \phi, z) = \frac{1}{4\pi}\sum_{k=1}^{N}\frac{\Omega_k}{|\mathbf{r}-\mathbf{r}_k|}, \tag{6}$$

$m=0$
$H_{\rho}^{(0)}(\rho,\phi,z) = -\frac{1}{4\pi^2}\sum_{k=1}^{N}\frac{\Omega_k}{\sqrt{\rho\rho_k}}\bullet \left[\frac{\partial}{\partial\rho}\left(Q_{-\frac{1}{2}}(\beta_k)\right) - \frac{1}{2\rho}Q_{-\frac{1}{2}}(\beta_k)\right]$ $H_{\phi}^{(0)}(\rho,\phi,z) = 0$ $H_{z}^{(0)}(\rho,\phi,z) = -\frac{1}{4\pi^2}\sum_{k=1}^{N}\frac{\Omega_k}{\sqrt{\rho\rho_k}}\bullet \left[\frac{\partial}{\partial z}Q_{-\frac{1}{2}}(\beta_k)\right]$
$m\geq 1$
$H_{\rho}^{(m)}(\rho,\phi,z) = -\frac{1}{2\pi^2}\sum_{k=1}^{N}\frac{\Omega_k}{\sqrt{\rho\rho_k}}\bullet \left\{\frac{\partial}{\partial\rho}\left(Q_{m-\frac{1}{2}}(\beta_k)\right) - \frac{1}{2\rho}Q_{m-\frac{1}{2}}(\beta_k)\right\}\cdot \cos\left[m(\phi-\phi_k)\right]$ $H_{\phi}^{(m)}(\rho,\phi,z) = -\frac{1}{2\pi^2}\sum_{k=1}^{N}\frac{q_k}{\sqrt{\rho\rho_k}}\bullet \left[\frac{1}{\rho}Q_{m-\frac{1}{2}}(\beta_k)\bullet \frac{\partial}{\partial\phi}\left(\cos\left[m(\phi-\phi_k)\right]\right)\right]$ $H_{z}^{(m)}(\rho,\phi,z) = -\frac{1}{2\pi^2}\sum_{k=1}^{N}\frac{\Omega_k}{\sqrt{\rho\rho_k}}\bullet \frac{\partial}{\partial z}\left(Q_{m-\frac{1}{2}}(\beta_k)\right)\bullet \cos\left[m(\phi-\phi_k)\right]$

Table 1: Magnetic field intensity components

where $\Omega_k(amperes\cdot meters)$ are the hypothetical magnetic charges. The units for magnetic scalar potential are in *amperes*.

From (4), (5), and (6), one can compute the corresponding magnetic scalar potential at some observation point given in cylindrical coordinates. This is written as

$$\Phi_P(\rho,\phi,z) = \frac{1}{4\pi^2}\sum_{k=1}^{N}\frac{\Omega_k}{\sqrt{\rho\rho_k}}\sum_{m=0}^{\infty}\epsilon_m Q_{m-\frac{1}{2}}(\xi_k)\bullet \cos\left[m(\phi-\phi_k)\right], \quad (7)$$

where $\xi_k = \frac{\rho^2+\rho_k^2+(z-z_k)^2}{2\rho\rho_k}$. The magnetic field intensity at any point in space external to the charged cylinder can be found from

$$\mathbf{H} = -\nabla\Phi_P(\rho,\phi,z), \quad (8)$$

where the gradient is taken in cylindrical coordinates. The magnetic components of $\mathbf{H}_P(\rho,\phi,z)$ can be tabulated for quick reference as shown in Table 1

VALIDATION

EXAMPLE 1 : Consider a permanent magnet centered at the origin and oriented along the x-axis with a magnetization given by $\mathbf{M} = M\hat{i}$ as shown Figure 4.

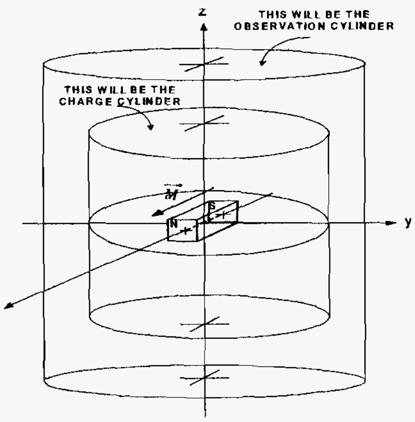

FIGURE 4 A cylindrical charged source

This example is based upon the author's research in permanent magnet motors. In particular, it was shown by Selvaggi *et al.* (2004) that the external field from permanent magnet motors can be determined by employing charge simulation. If the magnet is cubic in shape, with a side of length 0.1 m, and centered inside a hypothetical cylinder(*charge cylinder)* then the application of charge simulation will produce hypothetical magnetic charges at selected grid points on the cylinder. In other words, the magnet is replaced with an equivalent point charge distribution on a cylinder and this charge distribution is used to calculate the scalar potential using (7) on another hypothetical cylinder (*observation cylinder*) located outside and concentric to the charged cylinder. Employing (8) gives the magnetic field intensity external to the charged cylinder.

Let the charged cylinder have a maximum radius, $\rho_{\max}$, of 1 m, and a length, L, of 3.0 m, and let the magnetization, $|\mathbf{M}|$, of the magnet be 10^5 A/m in the x-direction as shown in Figure 4. Figure 5 is a plot of the magnetic scalar potential on the observation cylinder for the $m = 1$ term in (7). This cylinder has a length of 3.5 m and a maximum radius of 1.5 m. The $m = 1$ component turns out to be the dominant contributor to the magnetic scalar potential. The components m = 2, 3, 4 and higher contribute substantially less to the total potential. Figures 6 – 8 are the components of the magnetic field intensity for the m = 1 component.

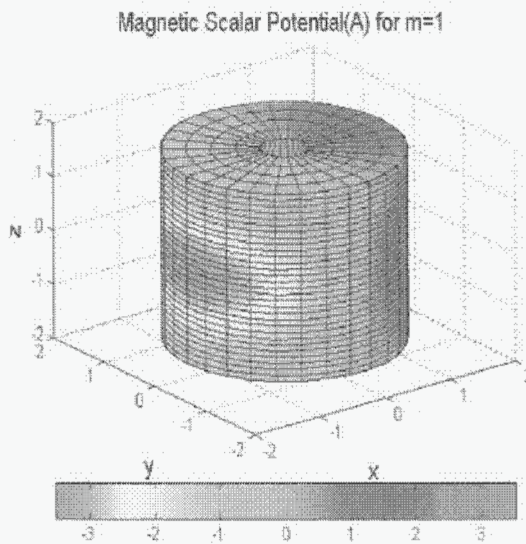

FIGURE 5

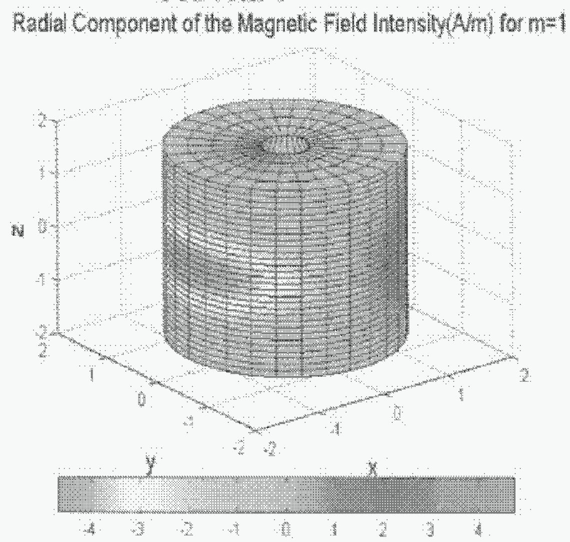

FIGURE 6

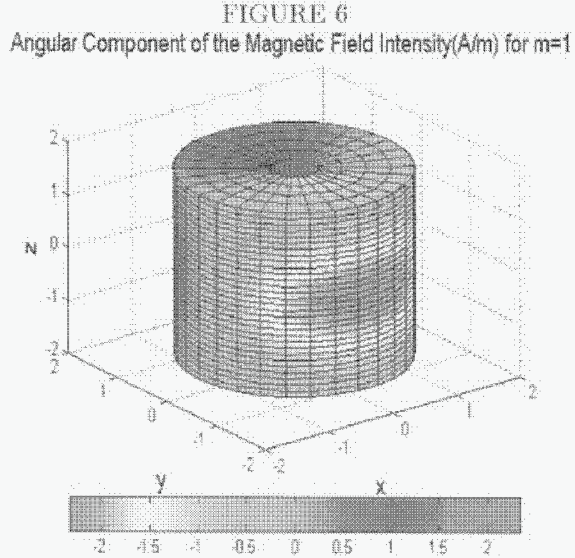

FIGURE 7

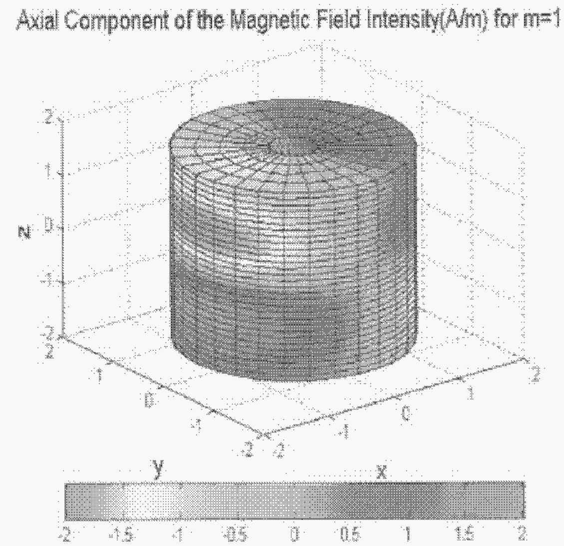

FIGURE 8

The charge index, k, in (7) ranges over all the charges. For this example, a total of 1230 charges were used; 930 on the cylindrical wall, and 150 charges per cap shown in Figure 2. The total magnetic scalar potential on the observation cylinder, produced from the permanent-magnet source, can be approximated by

$$\Phi(\rho,\phi,z) \simeq \Phi_P^{(1)}(\rho,\phi,z) = \frac{1}{2\pi^2}\sum_{k=1}^{N}\frac{\Omega_k}{\sqrt{\rho\rho_k}}Q_{\frac{1}{2}}(\beta_k) \bullet \cos(\phi-\phi_k), \tag{9}$$

where, for this example, $\rho = 1.5\ m$ on the observation cylinder's wall and $0.3\ m \le \rho \le 1.5\ m$ on the observation cylinder's caps. Likewise, $z = \pm 1.75\ m$ on the observation cylinder's caps, and $-1.75\ m \le z \le 1.75\ m$ on the observation cylinder's wall.

If one desires greater accuracy, then (7) must be used to retain contributions for all $m \geq 1$. Of course, depending on the magnetic source, not all of the Q-functions will contribute. When hypothetical magnetic charges are the source of the magnetic field then there will never be a $m = 0$ contribution since this would require that a monopole field existed which would contradict $\nabla \cdot \mathbf{B} = 0$. For electrostatic sources, a $m = 0$ term may or may not contribute.

EXAMPLE 2 : This example considers the calculation of the mutual inductance between two non-coplanar, parallel, and infinitely thin current loops, shown in Figure 10, by employing Q-functions. Consider first a single uniform current loop shown in Figure 9.

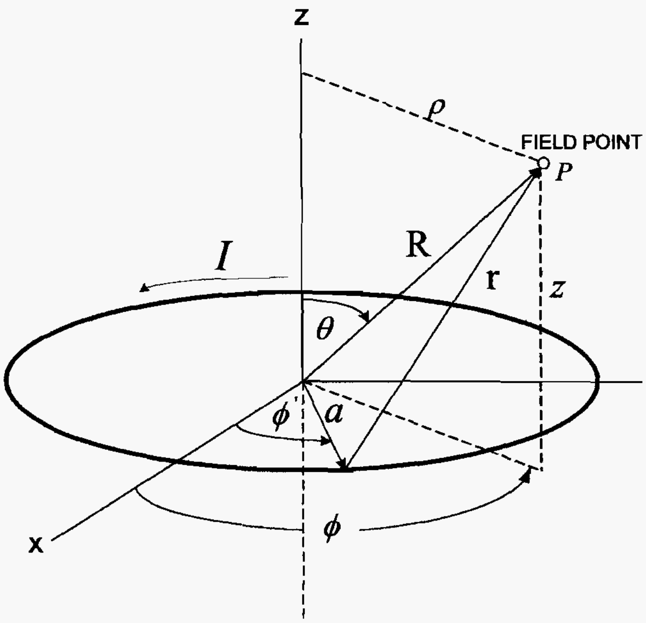

FIGURE 9 Filamentary current loop

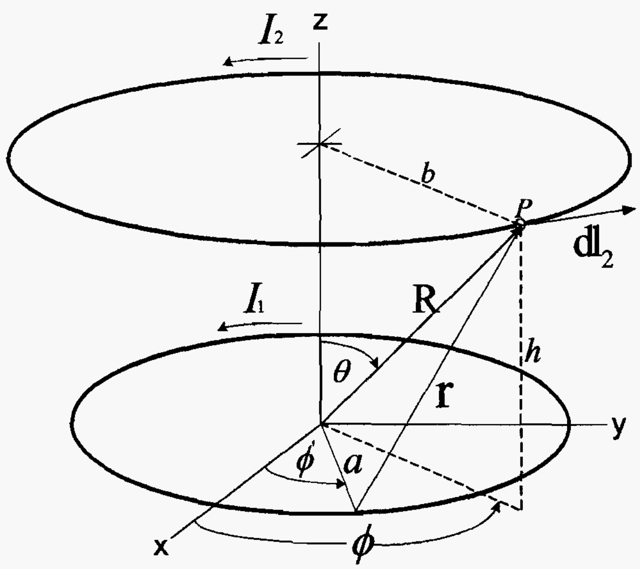

FIGURE 10 Two filamentary current loops

The differential magnetic vector potential at the field point, P, is given by

$$d\mathbf{A}_1 = \frac{\mu_0 I}{4\pi} \frac{a d\phi_1^{'}}{|\mathbf{R}-\mathbf{a}|} \widehat{\phi_1^{'}}, \qquad (10)$$

where

$$\frac{1}{|\mathbf{R}-\mathbf{a}|} = \frac{1}{\sqrt{\rho^2 + a^2 + z^2 - 2a\rho\cos(\phi - \phi_1^{'})}}. \qquad (11)$$

The magnetic vector potential at some arbitrary point in space not coincident with the current loop can be written as

$$\begin{aligned} \mathbf{A}_1(\rho,\phi,z) &= \frac{\mu_0 I a}{4\pi} \int_0^{2\pi} \left[-\sin(\phi_1^{'})\widehat{\imath} + \cos(\phi_1^{'})\widehat{\jmath} \right] \bullet \\ &\quad \frac{d\phi^{'}}{\sqrt{\rho^2 + a^2 + z^2 - 2a\rho\cos(\phi - \phi_1^{'})}}, \end{aligned} \qquad (12)$$

where the unit vector, $\widehat{\phi_1^{'}}$, has been replaced by its Cartesian equivalent. Using (4), the denominator of (12) can be written as

$$\begin{aligned} \frac{1}{|\mathbf{R}-\mathbf{a}|} &= \frac{1}{\pi\sqrt{\rho a}} \sum_{m=0}^{\infty} \epsilon_m Q_{m-\frac{1}{2}}(\xi_1) \bullet \\ &\quad \cos\left[m \left(\phi - \phi_1^{'} \right) \right], \end{aligned} \qquad (13)$$

where $\xi_1 = \frac{\rho^2+a^2+z^2}{2a\rho}$. Substituting (13) into (12) yields:

$$\begin{aligned} \mathbf{A}_1(\rho,\phi,z) &= \frac{\mu_0 I a}{4\pi^2} \frac{1}{\sqrt{\rho a}} \sum_{m=0}^{\infty} \epsilon_m Q_{m-\frac{1}{2}}(\xi_1) \bullet \\ &\quad \int_0^{2\pi} \left[\left(-\widehat{\imath}\sin(\phi_1^{'}) + \widehat{\jmath}\cos(\phi_1^{'}) \right) \bullet \right. \\ &\quad \left. \cos\left[m\left(\phi - \phi_1^{'} \right) \right] \right] d\phi_1^{'}. \end{aligned} \qquad (14)$$

Equation (14) is integrated to

$$\mathbf{A}_1(\rho,z) = \frac{\mu_0 I}{2\pi} \sqrt{\frac{a}{\rho}} Q_{\frac{1}{2}}(\xi_1)\,\widehat{\phi}. \qquad (15)$$

Equation (15) is also derived in Snow (1954). Equation (15) gives a mathematically alternative form for the magnetic vector potential valid for any arbitrary field point not coincident with the source. Using (5) with $m=1$, $Q_{\frac{1}{2}}(\xi)$ can be represented by the series

$$Q_{\frac{1}{2}}(\xi_1) = \frac{\pi}{2(2\xi_1)^{\frac{3}{2}}} \sum_{n=0}^{\infty} \frac{(4n+1)!!}{2^{2n} n!(n+1)!} \frac{1}{(2\xi_1)^{2n}}. \qquad (16)$$

The magnetic vector potential is now given by

$$\begin{aligned} \mathbf{A}_1(\rho,z) &= \frac{\mu_0 I}{4} \frac{a^2\rho}{(\rho^2+a^2+z^2)^{\frac{3}{2}}} \sum_{n=0}^{\infty} \frac{(4n+1)!!}{2^{2n} n!(n+1)!} \bullet \\ &\quad \left(\frac{a\rho}{\rho^2+a^2+z^2} \right)^{2n} \widehat{\phi}. \end{aligned} \qquad (17)$$

A few terms in the expansion are

$$\begin{aligned} \mathbf{A}_1(\rho,z) = \frac{\mu_0 I}{4} \frac{a^2\rho}{(\rho^2+a^2+z^2)^{\frac{3}{2}}} \Bigg[1 + \\ \frac{1\cdot 3\cdot 5}{2^2\cdot 1!\cdot 2!} \left(\frac{a\rho}{\rho^2+a^2+z^2} \right)^2 + \\ \frac{1\cdot 3\cdot 5\cdot 7\cdot 9}{2^4\cdot 2!\cdot 3!} \left(\frac{a\rho}{\rho^2+a^2+z^2} \right)^4 + \cdots \Bigg] \widehat{\phi}. \end{aligned} \qquad (18)$$

In order to make a comparison with a known solution, convert (18) to spherical coordinates. The coordinate transformation equations are

$$\rho = R\sin(\theta), \tag{19}$$
$$z = R\cos(\theta), \tag{20}$$
$$R^2 = \rho^2 + z^2. \tag{21}$$

If one substitutes (19), (20), and (21) into (18), the resulting expansion becomes

$$\mathbf{A}_1(R,\theta) = \frac{\mu_0 I}{4}\frac{a^2 R\sin(\theta)}{(a^2+R^2)^{\frac{3}{2}}}\left[1+ \frac{1\cdot 3\cdot 5}{2^2\cdot 1!\cdot 2!}\left(\frac{aR\sin(\theta)}{R^2+a^2}\right)^2 + + \frac{1\cdot 3\cdot 5\cdot 7\cdot 9}{2^4\cdot 2!\cdot 3!}\left(\frac{aR\sin(\theta)}{R^2+a^2}\right)^4 + \cdots\right]\hat{\phi}. \tag{22}$$

Equation (22) is identical to the Elliptic Function expansion given by Jackson (1999) on pages 182-183.

The mutual inductance between two non-coplanar, coaxial, and parallel current loops can now be computed. Using (16) with $\xi_1 = \frac{b^2+a^2+h^2}{2ab}$ and assuming $I_1 = I_2 = I$, the mutual inductance between the two current loops shown in Figure 10 is given by

$$\begin{aligned} M_{12} &= \frac{1}{I}\int_0^{2\pi} \mathbf{A}_1 \cdot d\mathbf{l}_2, \\ &= \frac{\mu_0}{2\pi}\sqrt{\frac{a}{b}}Q_{\frac{1}{2}}\left(\frac{b^2+a^2+h^2}{2ab}\right)\int_0^{2\pi} b\,d\phi_2, \\ &= \mu_0\sqrt{ab}\,Q_{\frac{1}{2}}\left(\frac{b^2+a^2+h^2}{2ab}\right). \end{aligned} \tag{23}$$

Equation (23) can be expanded to yield:

$$M_{12} = \frac{\pi\mu_0}{2}\frac{a^2b^2}{(a^2+b^2+h^2)^{\frac{3}{2}}} \bullet \sum_{n=0}^{\infty}\frac{(4n+1)!!}{2^{2n}n!(n+1)!} \bullet \left(\frac{ab}{a^2+b^2+h^2}\right)^{2n}. \tag{24}$$

Equation (24) represents the mutual inductance between two non-coplanar, coaxial, and parallel uniform current loops. Consider the case when $b = a$ and $h > 2a$. Imposing this condition yields:

$$\begin{aligned} M_{12} &= \frac{\pi\mu_0}{2}\frac{a^4}{(h^2+2a^2)^{\frac{3}{2}}}\left[1+\frac{1\cdot 3\cdot 5}{2^2 1! 2!}\frac{a^4}{(h^2+2a^2)^2} + \frac{1\cdot 3\cdot 5\cdot 7\cdot 9}{2^3 2! 3!}\frac{a^6}{(h^2+2a^2)^4}+\cdots\right] \\ &= \frac{\pi\mu_0 a}{2}\left[\left(\frac{a}{h}\right)^3 - 3\left(\frac{a}{h}\right)^5 + \frac{75}{8}\left(\frac{a}{h}\right)^7 + \cdots\right] \end{aligned} \tag{25}$$

Equation (25) is identical to the solution given by Jackson (1999) in problem 5.34 on page 234. Figure 11

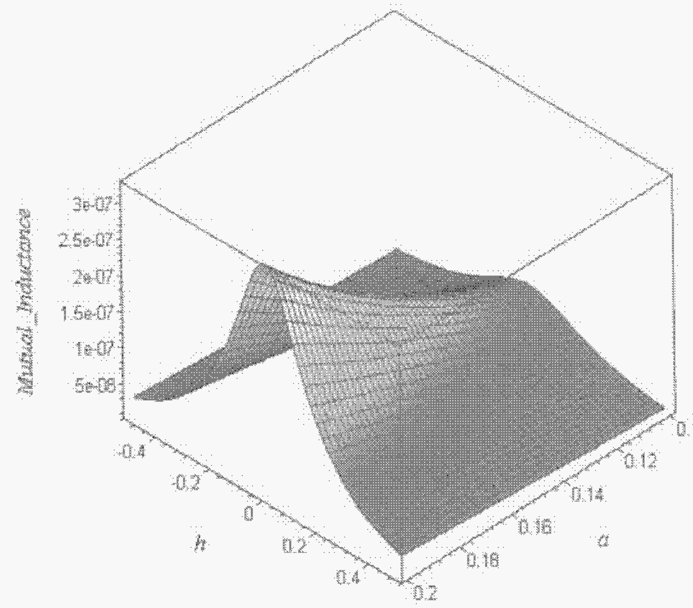

FIGURE 11 Mutual inductance of two current loops

shows the plot of (23) for $b = 0.3m$, and with $0.1m \le a \le 0.2m$ and $-0.4m \le h \le 0.4m$. The mutual inductance of the two current loop system shown in Figure 10 in terms of Elliptic integrals is given by

$$M_{12} = \mu_0\left\{\frac{(a^2+b^2+h^2)}{\sqrt{(a+b)^2+h^2}}K\left(2\sqrt{\frac{ab}{(a+b)^2+h^2}}\right) - \sqrt{(a+b)^2+h^2}\,E\left(2\sqrt{\frac{ab}{(a+b)^2+h^2}}\right)\right\}, \tag{26}$$

where $K(\cdot)$ and $E(\cdot)$ are complete Elliptic integrals of the first and second kind respectively. Of course, Figure 11 represents the plot of (26) for $b = 0.3m$. One may notice that (23) is in a much more mathematically compact form than (26).

DISCUSSION AND CONCLUSION

A general technique has been introduced for describing circular cylindrical magnetic systems. The Fourier series expansion or the toroidal expansion whose coefficients are the Q-functions can be used to represent a non-cylindrical magnetic source through the use of a method called charge simulation. These fictitious magnetic charges are located on a hypothetical cylinder which acts as the new magnetic source. Knowing the charge distribution on a cylinder greatly simplifies the mathematical problem since it allows one to immediately apply the magnetic form of Coulomb's law.

An example of a single permanent magnet was introduced in order to show how the charge simulation technique is applied. In particular, the toroidal expansion coupled with charge simulation allows one to accurately compute the far field from a circular cylindrical magnetic source where a purely finite element solution is known to be inaccurate. Another simple example was introduced in order to validate the toroidal expansion by comparing it to the solution found by a more well-known formulation. Specifically, the mutual inductance between two filamentary current loops was used to compare the known solution found in terms of an Elliptic integral with that found by using a toroidal expansion.

This paper has concentrated on a magnetostatic formulation, but there is a much wider range of topics for which the Q-function is applicable. For example, the Q-function can be applied to time-dependent magnetic field problems. Also, boundary value problems have not been studied in this paper. The Q-function formulation has been applied to problems whose boundary is at infinity. In fact, the free-space Green's function was directly used to formulate the inverse distance function in terms of a Fourier series expansion. However, all free-space Green's functions can be modified to handle finite boundaries. This would allow one to use a Q-function formulation where only a Bessel function approach existed. This adds another tool to the engineer's arsenal for tackling circular cylindrical electromagnetic problems.

The range of engineering applications which involve cylindrical geometries is immense. Areas such as electrodynamics, acoustics, continuum mechanics, dynamics of structures, and others can all benefit from adding another powerful mathematical tool which can be used to help solve problems which exhibit circular cylindrical symmetry. There is no theoretical reason prohibiting the application of the Q-function to electrodynamic problems such as electromagnetic radiation problems given in Overfelt (1996) and Werner (2000), eddy current formulations given in Hagel, Gong, and Unbehauen (1992), and Fawzi, Ali, and Burke (1983), and Dodd and Deeds (1968). Also, one could employ Q-functions for time varying electric and magnetic field formulations given by Lahart (2004) and Avilia (2003), etc. One could employ the Q-function formulation for computing electromagnetic forces in cylindrical coils shown in Kim *et al.* (1996) and Groom (1997). The author has already applied the Q-function approach to superconducting cylindrical disks given by Badia and Freyhardt (1998). These are just a few of the research areas which the author believes could benefit from a Q-function formulation.

References

Avila, M.A., "Magnetic fields of spherical,cylindrical, and ellipsoidal electrical charge superficial distributions at rotation," Revista Mexicana De Fisica, 49, April 2003.

Badia, A. and H.C. Freyhardt, "Meissner state properties of a superconducting disk in a non-uniform magnetic field," Journal of Applied Physics, Vol. 83, No. 5, March 1 1998.

Bouwkamp, C.J. and N.G. de Bruijn, "The Electrical Field of a Point Charge Inside a Cylinder, in Connection with Wave Guide Theory," Journal of Applied Physics, Vol. 18, June 1947.

Dodd, C.V. and W.E. Deeds, "Analytical Solutions to Eddy-Current Probe-Coil Problems," Journal of Applied Physics, Vol. 39, No. 6, May 1968.

Fawzi, T.H., K.F. Ali, and P. E. Burke, "Eddy Current Losses in Finite Length Conducting Cylinders," IEEE Transactions of Magnetics, Vol. Mag-19, No. 5, September 1983.

Groom, N.J., "Expanded Equations for Torque and Force on a Cylindrical Permanent Magnet Core in a Large-Gap Magnetic Suspension System," NASA Technical Paper, 3638, February 1997.

Hagel, R., L. Gong, and R. Unbehauen, "Evaluation of the Influence of a Finitely Long Circular Cylindrical Shield on the Electromagnetic Field," IEEE Transactions on Magnetics, Vol. 28, No. 5, September 1992.

Hobson, E.W., *On Green's Function for a Circular Disk, with applications to Electrostatic Problems,* Transactions of the Cambridge Philosophical Society, Vol. 18, 1900.

Jackson, J.D., *Classical Electrodynamics*, John Wiley and Sons, 3^{rd} ed., 1999.

Kim, Ki-Bong, E. Levi, Z. Zabar, and L. Birenbaum, "Restoring Force Between Two Noncoaxial Circular Coils," IEEE Transactions on Magnetics, Vol. 32, No. 2, March 1996.

Kwon, O-Mun, C.Surussavadee, M.V.K Chari, S.Salon, K.Sivasubramaniam, "Analysis of the Far Field Permanent Magnet Motors and study of effects of geometric asymmetries and unbalance in magnet design," IEEE Transactions on Magnetics, Vol. 40, March 2004.

Lahart, M.J.,"Use of electromagnetic scalar potentials in boundary value problems," American Journal of Physics, Vol. 72, No.1, January 2004.

Lebedev, N.N., *Special Functions and Their Applications*, Prentice-Hall, 1965.

Overfelt, P.L., "Near Fields of the Constant Current Thin Circular Loop Antenna of Arbitrary Radius," IEEE Transactions on Antennas and Propagation, Vol. 44, No. 2, February 1996.

Schwab, A.J. *Field Theory Concepts*, Springer-Verlag, 1988.

Selvaggi, J., S. Salon, O-Mun Kwon, M.V.K Chari, "Calculating the External Magnetic Field from Permanent Magnets in Permanent-Magnet Motors-An Alternative Method," IEEE Transactions on Magnetics, Vol. 40, NO. 5, September 2004.

Smythe, W.R., *Static and Dynamic Electricity*, McGraw-Hill, 3^{rd} ed., 1968.

Snow, C., *Formulas for Computing Capacitance and Inductance,* National Bureau of Standards Circular 544, September 1, 1954.

Snow, C., *Hypergeometric and Legendre Functions with Applications to Integral Equations of Potential Theory*, National Bureau Of Standards Applied Mathematics Series 19, U.S. Department of Commerce, May 1, 1952.

Snow, C., *Potential Problems and Capacitance for a Conductor Bounded by Two Intersecting Spheres*, U.S. Department of Commerce NBS, Research Paper RP2032, Vol. 43, October 1949.

Stratton, J. A, *Electromagnetic Theory*, McGraw-Hill Book Company, 1941.

Werner, D.H. and R. Mittra, *Frontiers in Electromagnetics*, IEEE Press, 2000.